MEASUREMENTS IN THE ATMOSPHERIC BOUNDARY LAYER : TECHNIQUES AND LIMITATIONS, REPRESENTATIVENESS

A. WEILL
CNET/CRPE/CNRS
38-40 rue du Général Leclerc
92131 ISSY-LES-MOULINEAUX (FRANCE)

Abstract: Different measurements useful for Atmospheric Boundary Layer simulation are presented. Our attention is drawn particularly to the problem of parameterization validity in the case of high order modelling.

1. INTRODUCTION

Theoreticians and experimentalists are often faced with the problem of measurements, whether it be for the initialization or validation of models or for analizing the physical processes highlighted by the measurements.

On the other hand, "parameterization" or normalisation is the tool that enables the experimentalist or theoretician to compare, understand various results corresponding to different experiments and, thus, to assess the consistency of the model or measurements.

If we consider the increasing complexity of models (ANDRE et al., 1976, 1978, 1979), we notice that the quantities to be measured are becoming increasingly sophisticated: from the altitude of the inversion layers Z_I, various fluxes (momentum, sensible heat, humidity), to moments of the second order, third order and even fourth order for studies on the dissymetry of vertical velocity distribution, as well as the essential measurements of turbulent dissipation rates or energy balances.

The aim of this article is, first of all, to review, albeit not comprehensively, the methods for measuring various parameters necessary for modelling, and also to show the validity of the measurements.

The following will be considered successively:

1) measurements of inversion altitudes,
2) measurements of fluxes (momentum, sensible heat, humidity).

With particular emphasis on:

3) measurements of turbulent dissipation rates,
4) measurements of vertical velocity variance and the moment of the third order on this variable,
5) estimates of budgets of turbulent kinetic energy, highlighting their implications for modelling.

2. MEASUREMENT OF THE RADIATION INVERSION ALTITUDE

This parameter plays a fondamental role in the dynamics of the boundary layer: Several methods of measurement are used.

1) Radiosondes typically give the intersection of the temperature sonde with the inversion, but in cases of rapid evolution or inversion oscillations, or when the inversion remains very close to the surface, results are questionable. In cases of very low level inversions, systems of "slow motion" low level soundings are preferable (HEISSAT et al., 1973).

2) A tethered balloon with a temperature probe is quite adequate to follow the evolution of the inversion altitude, at least in wind conditions below 15 ms^{-1}: this technique was used successfully by READING et al. (1972). Figure 1 shows the path of a probe fitted under a balloon and its advantage associated with an acoustic sounding: for each intersection with the inversion layer the variation of the thermal gradient gives the inversion altitude Z_I.

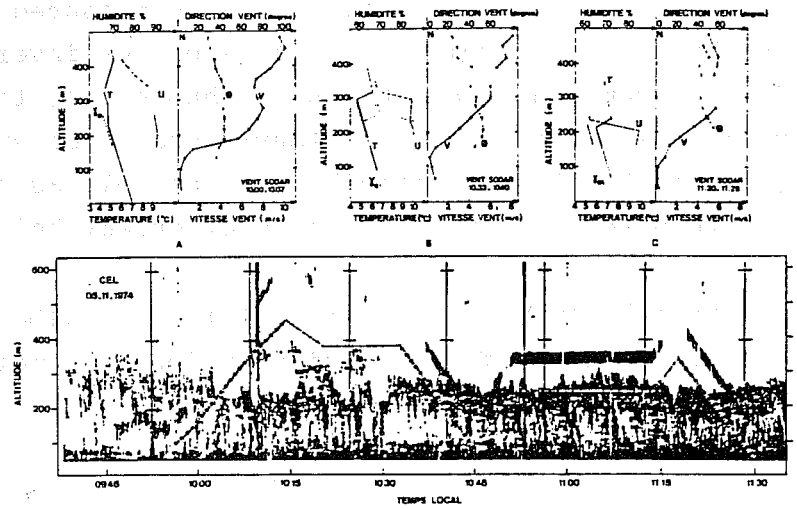

Fig. 1 Example of comparison between sodar recording (below) and atmospheric profiles obtained with a probe fitted under a tethered balloon (above). The probe path is indicated with a continuous line on the fac-simile. A, B and C profiles represent the 1000-1015 ascent and both 1035-1045 and 1117-1130 descent respectively. The position of echos recorded by sodar is indicated by the grey area on the profiles. Mean wind profiles were determined by sodar (ESTIVAL and AUBRY, 1975).

3) Aircrafts with adequate instruments on board may give the inversion altitude at several points in space, provided that during flight time its level remains almost constant: however, it happens fairly frequently that in about 10 minutes, which is the period for an average path of several kilometers, the morning inversion rises by several hundred metres (morning transition). Thus, the aircraft gives a space representation of the inversion altitude during a time interval T on a path L = UT, U being the speed of the aircraft, which is assumed to be much greater than that of the atmospheric flow.

4) Acoustic soundings make it possible to monitor inversions, provided that they are associated with some thermal turbulence (in monostatic mode), AUBRY et al. (1975). On the other hand, and this can be seen on figure 1, the inversion altitude detected by acoustic sounding corresponds to the altitude of maximum "reflectivity" or backscattering intensity and is at an altitude near the base of the inversion, meaning the points where the temperature gradient becomes stable. Precision is linked with the space resolution of the instrument and is generally in the region of about 20 metres. Figure 2 shows a method of monitoring the inversion altitude by looking for maximum reflectivity: by this type of monitoring it is possible to determine the evolution of inversion layers on a much finer scale than that of most models.

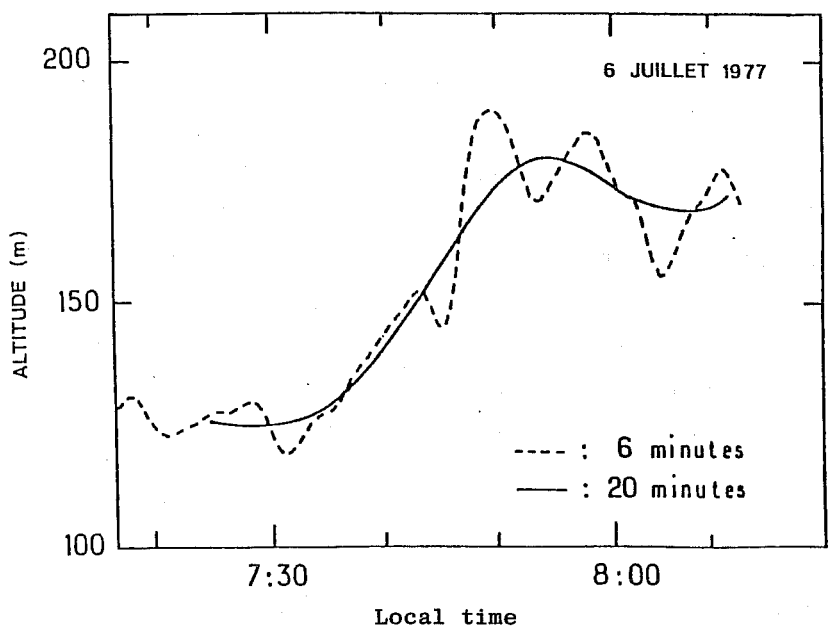

Fig. 2 Inversion ascent filtered over 6 and 20 minutes (Pierre Bouteloup's method of inversion monitoring).

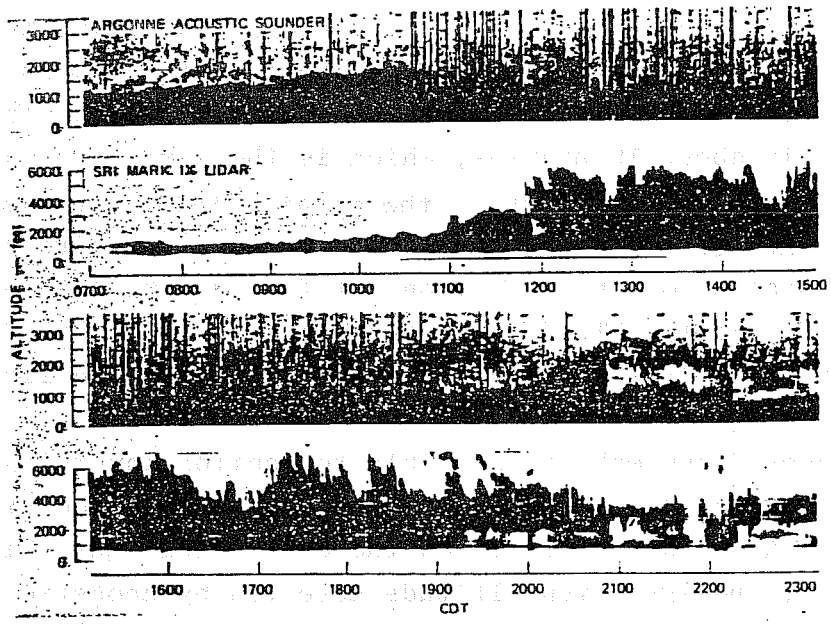

Fig. 3 Simultaneous recordings obtained by sodar and idar at Saint-Louis (Missouri) on 14 August 1972 from 7.20 to 23.00h local time. The congestion of pollutants in the mixed layer above 1000 m is clearly seen before 1100 m; their vertical diffusion due to convection shown by sodar is seen after 1100 m (RUSSELL et al., 1974).

5) LIDARs can be used also to assess an inversion altitude but its meaning is different from that given by sodar and corresponds to an altitude which could be indicated at Z_I, slightly below the sodar echo, which is a zone where aerosols are trapped. This remark is illustrated by figure 3., after RUSSEL (1974), showing an interesting comparison between sodar echo and LIDAR.

Generally speaking, it can be said that although inversion altitudes given by various instruments are different, they come near the inversion altitude as defined in the models by approximately 20 metres, except in cases where the inversion is very close to the ground and where it is difficult to define altitude Z_I: is it the low level jet altitude or the altitude of maximum acoustic reflectivity or some other altitude determined by the sounding? As regards the thickness of inversion layers, these direct temperature sounding methods are probably adequate to assess it correctly.

3. FLUX MEASUREMENTS IN THE SURFACE LAYER

FLUX MEASUREMENTS OF MOMENTUM

These measurements are derived for the most part from the use of various types of anenometers:

1) rotating anenometers,
2) hot wire anenometers,
3) acoustic or sonic anenometers.

Two methods are the most frequently used: direct measurement by correlation between the horizontal and vertical components of the velocity fluctuations, or the profile method (BUSINGER, 1971).

3.1 Direct calculation of $\overline{u'w'}$ by a method of correlation between sensors

The direct method for measuring correlation calls for the use of measuring instruments with very short response time. Noteworthy is the analogy between the 3 dB cut-off frequency and the response length: length of flow necessary for the response by the instrument to the flow velocity corresponding to the 3 dB cut-off frequency:

$$f_c = \frac{U}{l_r}$$

f_c = cut-off frequency

l_r = response length

On the one hand, a relatively long integration time is necessary for the contribution $\overline{u'w'}$ to be significant (WYNGAARD, 1972). Hot wire anenometers, GILL anenometers (u, v, w), sonic anenometers or triaxial ionic anenometers are all adequate.
In spite of the results obtained by DESJARDINS and LEMON (1973), which conclude that a time constant of 0.5s is sufficient to calculate the fluxes, GARRAT (1975) has shown that, in calculating fluxes,

$$F_s = \rho \overline{w's'} = \rho \int_0^\infty \Phi_{ws}(f)df \qquad (1)$$

where ρ is the air voluminal mass,
s' is the velocity or temperature disturbance,
ϕ (f) is the cospectral density

a cut-off frequency of several Hertz and an integration time longer than 15 minutes are necessary to integrate fluxes (figure 4). Measurements made with GILL type anenometers with a time constant of the order of 0.5s may underestimate the flows by 40%.

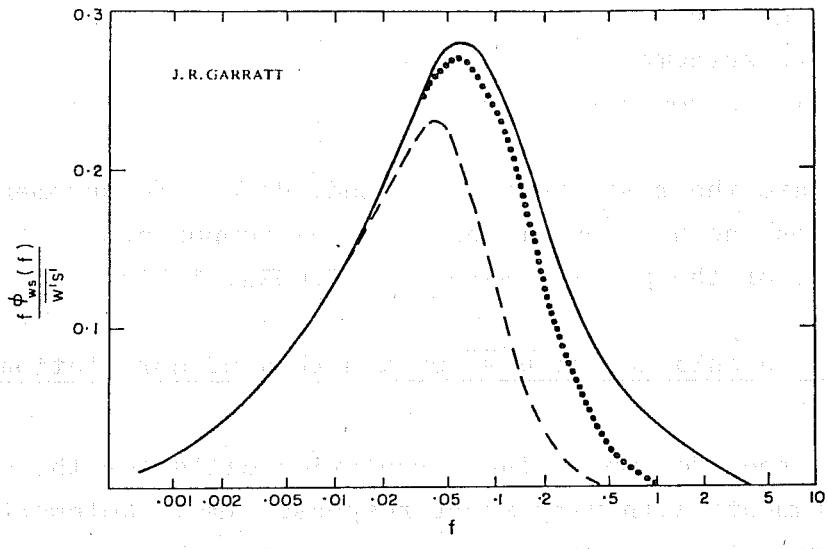

Fig. 4 Normalised cospectra for vertical velocity (w) and property (s) as a function of normalised frequency. Based on previous experimental results, cospectra probably apply for momentum, heat, water vapour and carbon dioxide transfer in near-neutral stability. Full line is perfect sensor response at all frequencies; dotted curve has time response (t) = 0.5 s, u = 5 m s^{-1} and z = 5 m; broken curve has t = 0.5 s, u = 5 m s^{-1} and z = 1.5 m.

In fact, the integration scales are justified by a careful analysis of the cospectral densities or covariances.

An additional difficulty may occur when eliminating secular components from the fluctuation components, especially when there are medium scale components.

Normally, measurement accuracy should reach 10%.

3.2 Calculation of momentum transfer by the PAULSON-BUSINGER method

This method is based on the consideration of the mean temperature field and the mean velocity in the surface layer derived from identical temperature and velocity gauges which are in general logarithmically spaced, with a basic asumption that the variability of the vertical fluxes in the surface layer does not exceed 10%: assuming a linear variation of the different fluxes such that $\phi = \phi_o \left(1 - \frac{Z}{Z_I}\right)$ (first approximation), a 10% variation corresponding to $Z/Z_I = .1$, a non-dimensional altitude fairly close to the so-called surface layer (S.L.).

Universal functions are very well described in the literature and we will not go into that, but we will assume that these similarity laws are known to within 10%: under conditions of instability, fluxes may be estimated (u_*, $\theta_* = Q_o/u_*$), to within 20%, taking into account that the various errors or uncertainties are independant and that allowance has been made for the 10% flux variability in the surface layer.

Under highly stable conditions of sporadically stratified boundary layer, it seems that the universal functions have to be reassessed and a direct measurement then seems to be much more appropriate, provided that the vertical velocity can be assessed correctly (hot wire or sonic anenometer).

Generally speaking it is not so much the measuring of u_* that presents a problem, but more its representativeness: if measured too close to the ground, the vertical transfer of horizontal momentum is subject to the characteristics of the "point of measurement", and the higher the altitude of measurement within the surface layer, the more representative of a large volume will the measured u_* be (WIERINGA, 1980). To that effect, KLAPISZ and WEILL (1978) have proposed a method of measurement based on data from the top of the surface layer and from the bottom of the convective layer, and this shows that the range of u_* measurements, as well as of those of roughness length Z_o, are quite different from the range of measurements at ground level, but that they are well correlated in time variations.

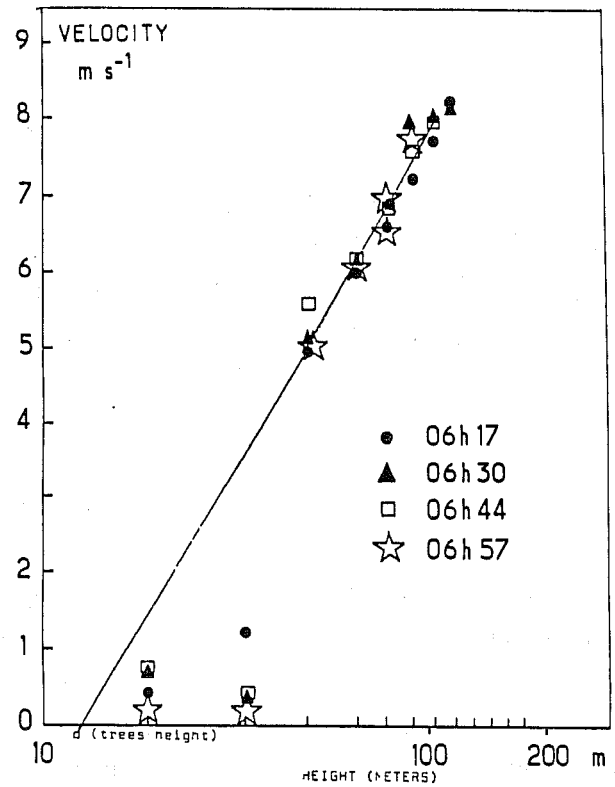

Fig. 5

The presence of obstacles, hedges, small relief, alters the wind profile and consequently $u_* Z_o$; it is,therefore, necessary to introduce before Z_o a displacement length d.

Doppler echo sounders can be used to measure this displacement effect (figure 5).

If turbulence conditions are stationary, the direct measurement method seems to be the most reliable, but in non stationary conditions, the profile method is preferable, provided of course that profiles have been measured over a sufficiently long period of time T to allow integration of all production ranges. In the profile method, accuracy is of the order of 25%.

3.3 Turbulent transfer of sensible and latent heat

The profile method has already been mentioned in the preceding paragraph. Although it is justified to use it to calculate the fluxes of momentum and sensible heat, it is preferable to couple the measurements of temperature and velocity gradients with that of the net radiation, as humidity gradients are difficult to measure correctly.

Net radiation = H (sensible heat flux) + LE (evaporation flux)
+ G (ground flux).

Net radiation is obtained with a radiometer.
G is derived from measurements of the thermal gradient in the ground implying that the heat conductivity of the ground is known.
H is deduced from the profile method and LE is deduced from that.

The method using the BOWEN ratio seems rather inaccurate, because of the difficulty in measuring humidity gradients accurately; and only maximum evaporation can be calculated by the lisymeter method.

Instruments have been developed for the direct calculation of fluxes by the net radiation method = at I.N.R.A. (Institut National de la Recherche Agronomique (FRANCE)), PERRIER et al. (1976) have developed the B.E.A.R.N. system for this purpose : flux accuracy is of the order of 30%. During the VOVES experiment (1977), where several methods and measurement points of flux (over homogeneous ground) were used, differences of 40% were found between measurements (Fig. 6) (ANDRE et al., 1981). When convective conditions are $-\frac{Z}{L} \geq 2$, L being the MONIN-OBUKHOV length, the variance of the sodar vertical velocity makes it possible

to obtain an estimated heat flux representative of a greater atmospheric volume than the measurement at ground level (WEILL et al. 1981).

$$\frac{\sigma_w^3}{z} = A \frac{g}{\theta} \overline{w'\theta'_v} \quad \text{for} \quad -\frac{z}{L} \gg 2 \qquad (2)$$

Net energy, albedo, net radiation.

A = constant

g = gravity acceleration

z = altitude

σ_w = standard deviation of vertical velocity

$\overline{w'\theta'_v}$ = flux of virtual temperature

$\overline{\theta}$ = mean potential temperature

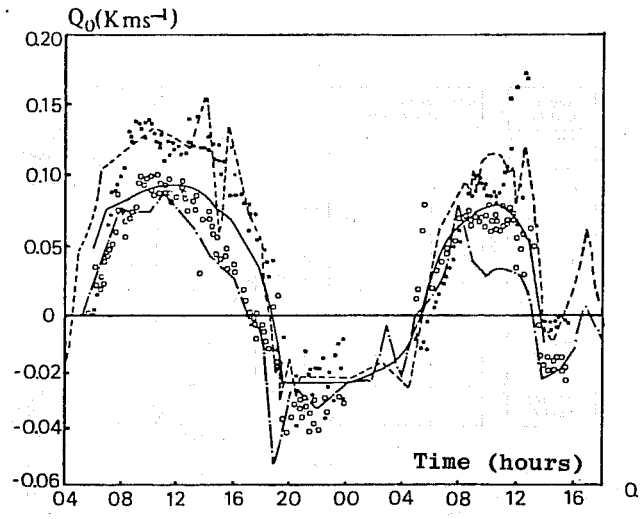

Fig. 6 Different estimates of heat flux Q_o :

(----- : inversion of universal laws from the 10 m. mast;
—·—·— : BEARN method; oooo BOWEN ratio method;
..... : aerodynamic method)
——— : evolution used in the model

(from Andre and Lacarrere, 1980)

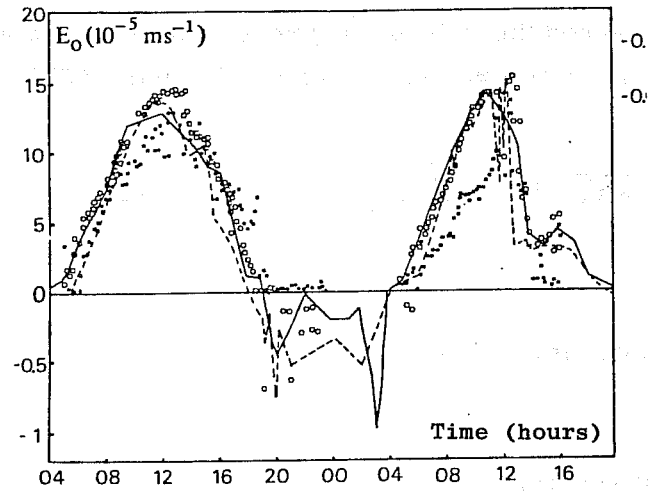

Different estimates of humidity flux E_0: same symbols; the full lines represent the results of the BEARN method which is used directly in the model.

Fig. 7 illustrates the advantage of such a method for measuring the flux profiles necessary for the study of the atmospheric boundary layer (A.B.L.) evolution. As for measuring directly humidity fluxes, the use of Lyα absorption is an interesting tool (COANTIC and LEDUCQ, 1969), but this technique is still difficult to master.

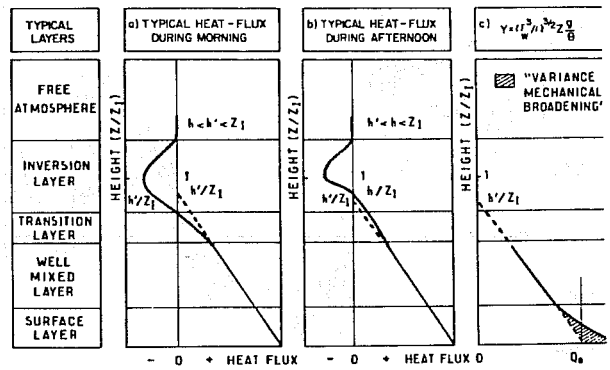

Typical heat flux profiles during convective activities: (a) during morning $h < h' < Z_i$ (shall convection), where h is the height of zero heat flux, h' is the height of zero heat flux obtained linear extrapolation, and Z_i is the height of maximum negative heat flux; (b) during afternoon (v developed convection) $h' < h < Z_i$; (c)

$$Y = \sigma_w^3 \left|\frac{g}{\bar{\theta}}\right|^{-1} \alpha^{-3/2} z^{-1} \approx \left|\frac{g\delta}{\bar{\theta}}\right|^{-1} \bar{U}^2 \frac{d\bar{U}}{dz} + Q_0$$

giving h'/Z_i and Q_0. Note that the hatched part corresponds to a "variance broadening" due mechanical production.

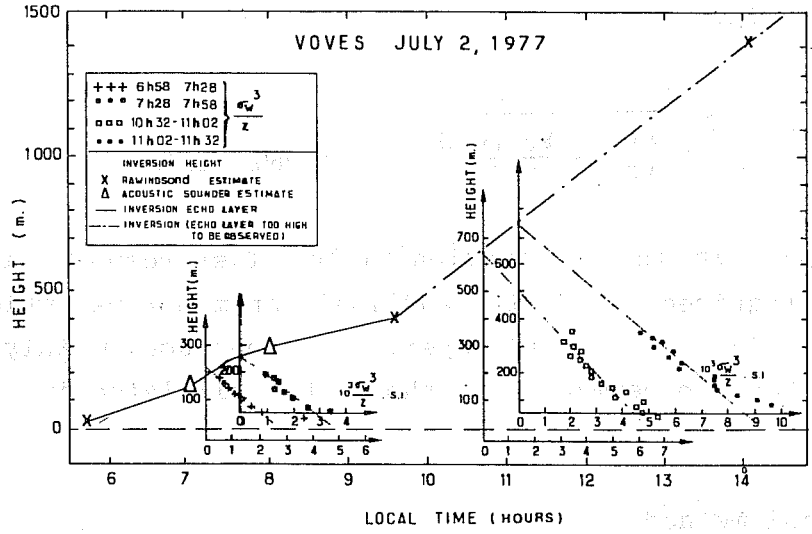

Fig. 7 Variation of inversion height and σ_w^3/Z profiles, 2 July 1977 at Voves, France.

4. MEASUREMENT OF THE TURBULENT DISSIPATION RATE

The dissipation rate is a crucial element in the parameterization of the turbulent kinetic energy within a size D mesh, such that if D is within the inertial range and if the turbulent kinetic energy is known, the dissipation rate can be calculated by applying the following:

$$\varepsilon = \frac{a(l)e^{3/2}}{l} \qquad (3)$$

where l is the dissipation length
a(l) is a constant depending on the flow stability.

However, it is necessary that at the size D, the inertial ranges of the longitudinal and transverse components are isotropic (ANDRE et al., 1981).

1) Direct measurement of dissipation rate

Theoretically, the turbulent dissipation rate is expressed as follows:

$$\varepsilon = \nu\overline{\left(\frac{\partial u_i}{\partial x_j} + \frac{\partial u_j}{\partial x_i}\right)\frac{\partial u_i}{\partial x_i}} \qquad (4)$$

ν = kinematic viscosity.

and the knowledge of 9 components is necessary, but in the case of isotropy carried out for the dissipation field, this formula is reduced

to the following:

$$\varepsilon = 6\nu\left(\overline{\frac{\partial u}{\partial x}^2} + \overline{\frac{\partial u}{\partial z}^2} + \overline{\frac{\partial u}{\partial z}\frac{\partial w}{\partial x}}\right) \quad (5). \text{ HINZE (1975)}$$

For measuring ε in the dissipation field, fast response anemometric systems are required. Hot wire and ionic anemometers, which are difficult to use in the boundary layer, have been used mainly in wind tunnels, although presumably ε should be calculated in the field of dissipation.

2) Inertial method

This is the most commonly used method; it has been the subject of much work: TSVANG (1963), (1969); READINGS and RAYMENT (1969) are examples of this. It consists in searching for correlation or structure functions of the longitudinal and transverse velocity disturbances of the flow velocity:

i.e.
$$D_{rr} = C\,\varepsilon^{2/3}(\Delta r)^{2/3}$$
$$D_{tt} = \frac{4}{3}\,C\,\varepsilon^{2/3}(\Delta r)^{2/3} \quad (6) \text{ KOLMOGOROV (1941)}$$

where D_{rr} and D_{tt} are respectively the structure functions of the longitudinal and transverse velocity fluctuations, D_r is the structure increment.
In fact, it should be pointed out that ε corresponds in this formula to a mean ε on the Δr measurement interval. C is the KOLMOGOROV constant equal to 1.8. These expressions have their equivalent in spectral density :

$$E_r = C\,\varepsilon^{2/3}\,k^{-5/3}$$
$$E_t = \frac{4}{3}\,C\,\varepsilon^{2/3}\,k^{-5/3} \quad (7)$$

where k = wave number = $\frac{2\pi f}{V}$

f = time frequency, V = mean flow velocity.

Both methods have been used concurrently; they allow to obtain only ε; however, whereas it is possible to obtain ε under various conditions by the correlation method, even when the wind is light, this is not possible by the spectral method. Measurement accuracy may be below 30%.

Nevertheless, the non-stationary nature of the turbulent dissipation rate must be taken into account : if one is interested in variability, short intervals will be taken, but estimation will be poor.
One way of validating the measurement of ε will be to include it in the budgets or to compare it with the WYNGAARD and COTE (1971) similarity formulae:

$$\varepsilon = \frac{u_*^3}{hZ}\left(1 + 0.5\left|-\frac{z}{L}\right|^{2/3}\right)^{3/2} \qquad (8)$$

$$\varepsilon = \frac{u_*^3}{hZ}\left(1 + 2.5\left(\frac{z}{L}\right)^{3/5}\right)^{3/2}$$

The disadvantage of the inertial method is that it can reveal an anisotropy in the measurements of the components of the turbulent dissipation rate (Fig. 8)and that when the differences between ε, as measured

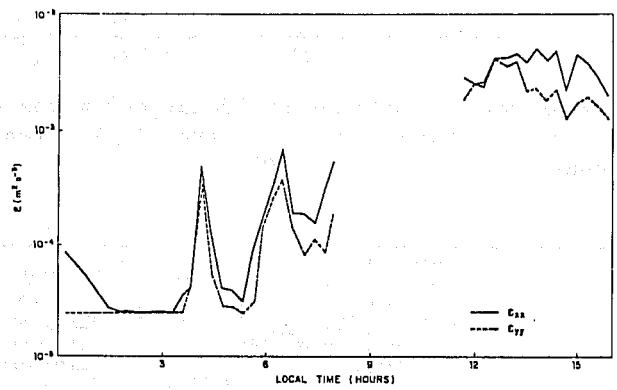

Fig. 8a Longitudinal and transverse dissipation rates at 72m, for 23/11/78.

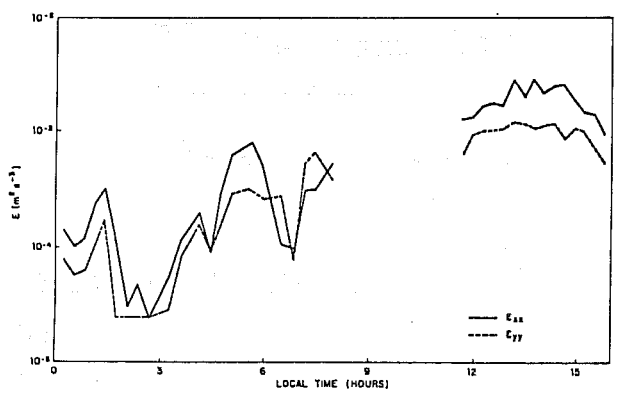

Fig. 8b Same as (a), but for 18m.

longitudinally and transversely,are greater than the measurement error, this must be taken into account in the parameterization at the D-grid scale. It has been possible to measure systematically the dissipation rate by acoustic soundings in the thin atmospheric boundary layer (GAYNOR, 1976; WEILL et al. 1976; WEILL et al. 1978).
Of course, the uncertainty is great, 40%. On the other hand, we have followed the evolution of this value in the whole of the boundary layer and the differences in the measurements are interesting: (Fig. 9).

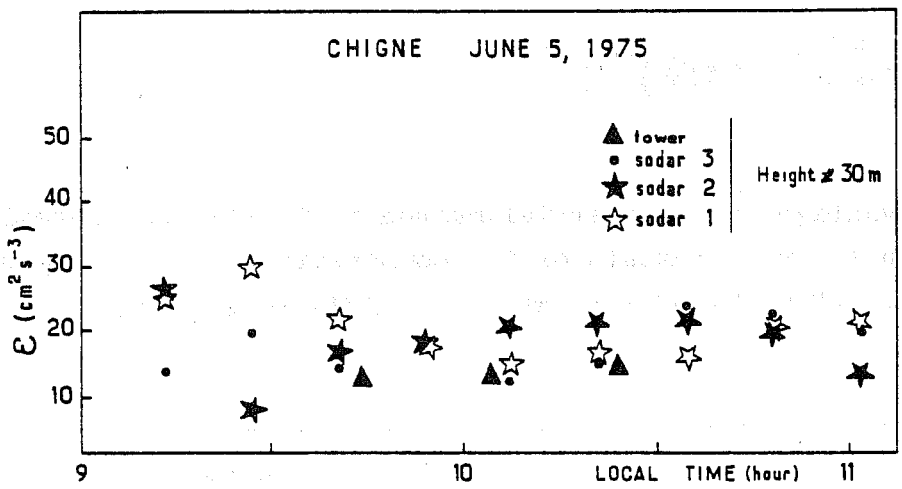

Comparison between tower estimates and sodar estimates of ε with the three-antenna system (30-m altitude), 3 (vertical antenna), 2 and 1 slanting antennas, Chigne, 5 June, 1975.

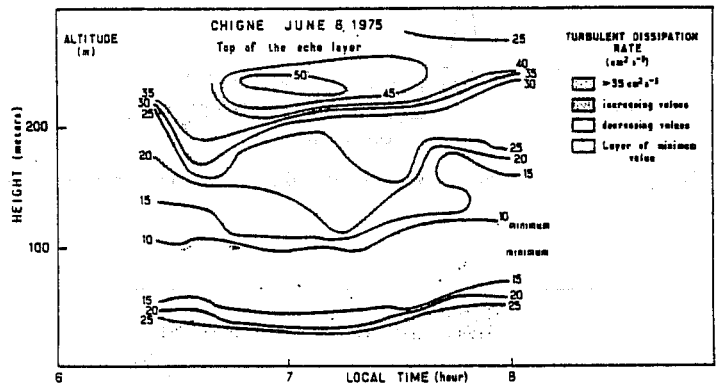

Fig. 9 Isopleths of dissipation rate (ε $cm^2 s^{-3}$), Chigne, 6 June, 1975.

5. MEASUREMENT OF THE VERTICAL VELOCITY VARIANCE

Sonic, ionic, hot wire anemometry, vane or cup anemometers can provide measurements of vertical velocity, as well as variances of vertical velocity.
For variance measurements to be accurate, they must take into account the whole of the energy scales (mainly the small scales).

Fig. 10 shows the differences between measurements taken by aircraft and measurements taken by sodar : it can be seen that the lack of accuracy of the measurements are mainly connected with the representativeness of the various measurements. Indeed, the effects of space heterogeneities are taken into account in the aircraft path whereas sodar records the passage of the "frozen" turbulence and, because of the sodar response frequency, 80% of the true variance is obtained (WEILL et al., 1980; CAUGHEY et al., 1981).

CAUGHEY ET AL 1980

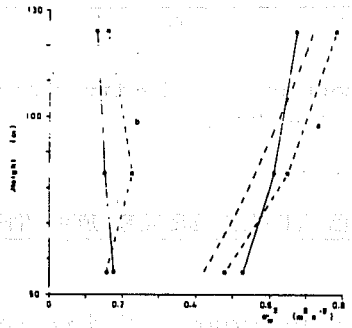

Fig. 17. Vertical profiles of the vertical velocity variance within the range $2 \times 10^{-4} < n < 2 \times 10^{-2}$ Hz from the turbulence probe ○ and acoustic sounder ● for (a) Run 1 and (b) Run 2 on 29 April 1976.

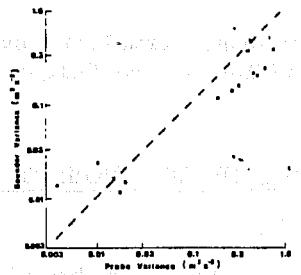

Fig. 19. Comparison of sounder and turbulence probe velocity variances. Vertical velocity, convective conditions (0·0003–0·07 Hz) ● Vertical velocity, stable conditions (0·0003–0·02 Hz) ○. Horizontal velocity in the plane of the bistatic sounder, convective conditions + and stable conditions ■.

VAN GRUNDERBEECK 1978

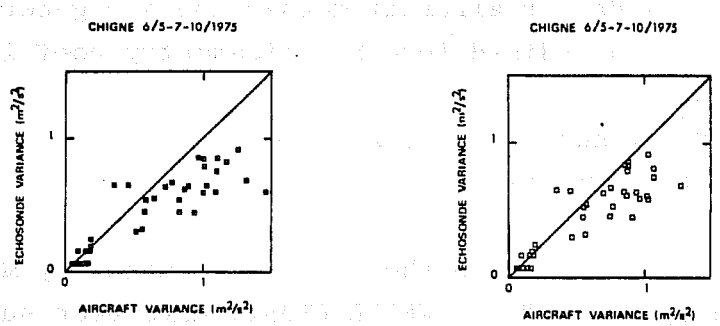

TACONET AND WEILL 1981

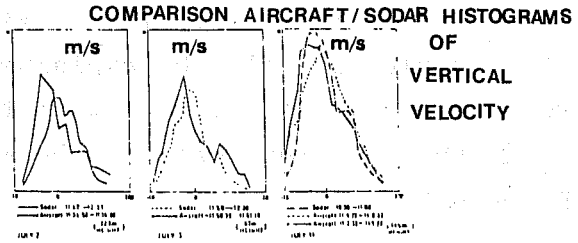

Fig. 10

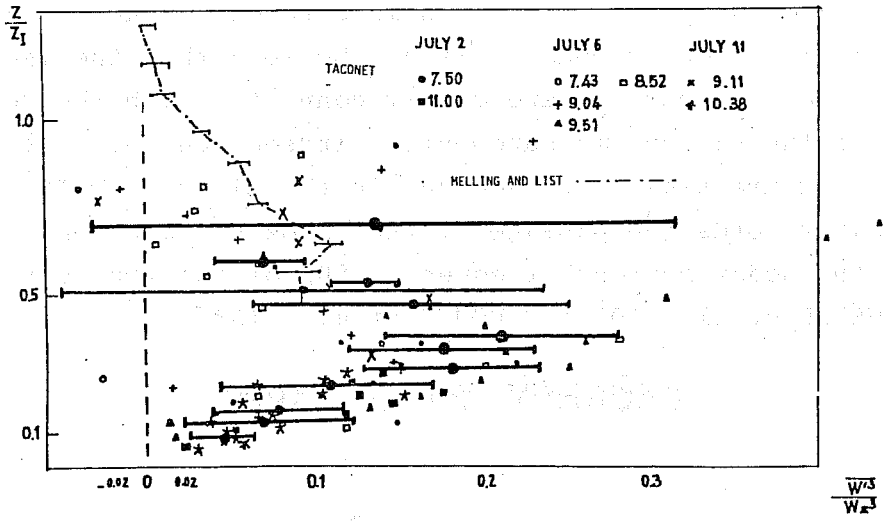

Fig. 11 Skewness, normalized by the convective velocity scale W_*, as a function of the height normalized by Z_I.

6. MEASUREMENT OF THE MOMENT OF THE THIRD ORDER FOR THE VERTICAL VELOCITY w'^3

Profiles of this value can be obtained by means of instruments carried on board aircraft, sodar measurements, instruments placed in towers.

For these measurements to be significant, it is necessary also that the spectral density $E_{w'3}$ shows some energy at those frequencies corresponding to the sodar or aircraft measurements : generally $\overline{w'^3}$ is represented in a standardized form S = dissymetry coefficient = $\frac{\overline{w'^3}}{w_*^3}$, where $w_* = \frac{g}{T} Q_o Z_I$

Q_o = flux of virtual surface temperature

T = mean temperature in °K.

Experimentally, Fig. 11, where the results obtained by MELLING and LIST (1980) and by TACONET and WEILL (1981) have been superimposed, reveals a profile which is fairly close to that forecast by the models (ANDRE et al. 1981).

However, superimposition of the results from the latest experiments shows a dispersion which could partially be explained by the experimental conditions. Taking into account the fact that the turbulent dissipation rate $\varepsilon = \alpha \frac{g}{T} Q_o$ and that the term for the kinetic energy transport can be expressed as :

$$\frac{\partial}{\partial z}\left(.7 + .275\frac{z}{Z_I}\right)\overline{w'^3} = \frac{\partial}{\partial z}\,\overline{w'e'} \qquad (9) \quad \text{WILLIS et DEARDORFF (1975)}$$

we obtain, for typically $.2 \leq \frac{Z}{Z_I} \leq .6$,

$$\frac{\partial}{\partial z}\left(.7 + .275\frac{z}{Z_I}\right) \approx \frac{g}{T} Q_o \left(1 - \frac{z}{h}\right) \qquad (10)$$

where h is the level where the heat flux is cancelled ($h \leq Z_I$)

It can then be noted that the profile reaches its maximum when $Z_M = h(1-\alpha)$, with $\alpha = .5$, $Z_M \simeq .5h$.

As h is generally comprised between $0.6Z_I$ and Z_I, $.3 \leq Z_M \leq .5$ is obtained, which explains the spreading of the maximum.

In the case of the free convection alone, the following should obtain:

$$\frac{\overline{w'^3}_{max}}{w_*^3} \approx \frac{.125\frac{h}{Z_I}}{.7 + .275\frac{h}{Z_I}} \qquad (11)$$

which gives $h/Z_I = .9$.

$\frac{\overline{w'^3}_{max}^{\frac{1}{3}}}{w_*} \simeq .49$, a result which agrees well with the value of .5 which is forecast by the model of ANDRE et al. (1981).

It seems unreliable to want to mix arbitrarily the various experiments through normalisation, because of entrainment effects which appear at the level h; the experimental normalisation curves obtained by the method of least squares must be analysed carefully: in addition to presenting a normalised result, it is necessary to present gross results giving details on the conditions of the experiments.

To that purpose, experimental budgets of kinetic energy, temperature variance or humidity variance are excellent tools for analysing the results.

7. CONCLUSION AND BUDGET OF TURBULENT KINETIC ENERGY

Budgets correspond to what experimentalists and modelists must be able to measure, understand and forecast: they make it possible to use the data on turbulent kinetic energy, mean flow velocity, various moments, with a limited number of degrees of freedom.
On the other hand, budgets make it possible to analyse experimental conditions and, therefore, to select those parameters which are essential for parameterizing the elements of the budgets.

This is illustrated in Fig. 12A.; in the case of the CHIGNE and VOVES experiments, we are dealing with unstable layers with weak shear where the sensible heat flux is cancelled towards $0.8Z_I$ and the mechanic productions of shear are fairly weak.

A decrease in the turbulent dissipation can be seen, mainly in the afternoon, in the thick boundary layer. This result is well illustrated by the forecast obtained from the model of ANDRE et al. (1981) (Fig. 12B).
We have included the normalized turbulence kinetic energy balance in the case of a boundary layer with shear (PENNEL and LE MONE, 1973). A counter gradient shear production from $Z/Z_I=.3$ can be seen on this figure (Fig. 12C).
As far as budgets are concerned, it can be seen that measurements taken by aircraft and acoustic soundings are complementary and that it is necessary, in order to ensure consistency of measurements,

1) to have redundant measurements in a series of experiments,
2) to present measurements both in a gross and adimensional form, so that critical problems can be examined: zero-level flux, surface layer height, and
3) it is advisable to carry out profile measurements with instruments which are as similar as possible, which can be done in the case of acoustic remote sensing measurements.

In addition, it seems that the most important is not the accuracy of a measurement but its representativeness.

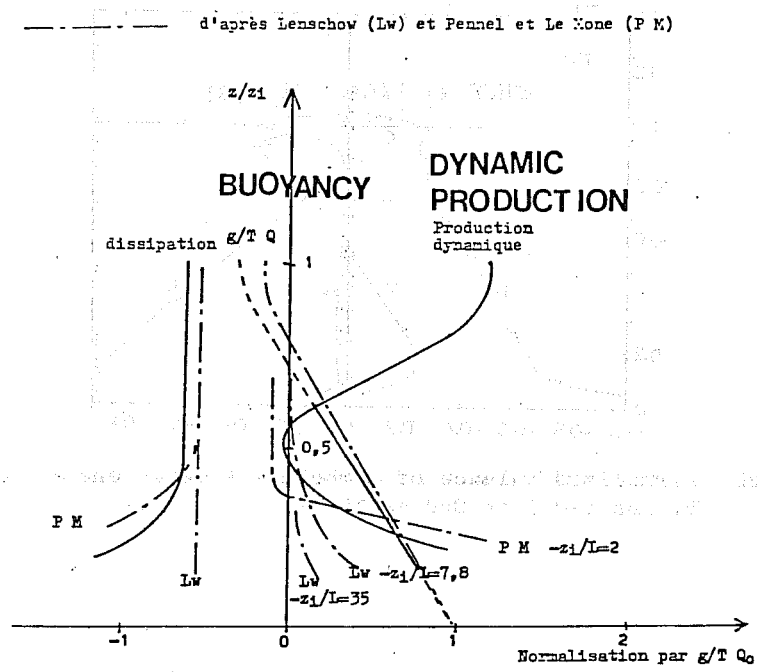

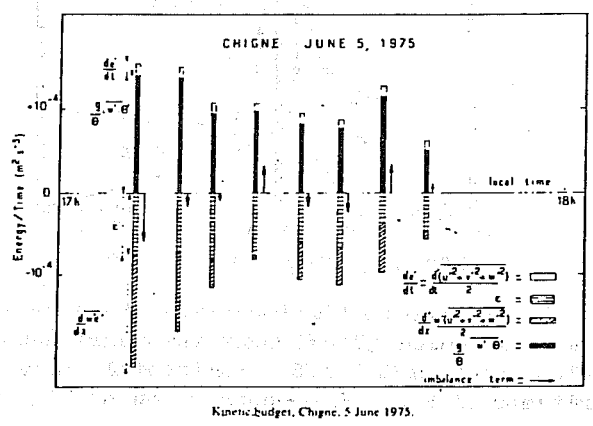

Kinetic budget, Chigne, 5 June 1975.

Fig. 12a (from Strauss,1980)

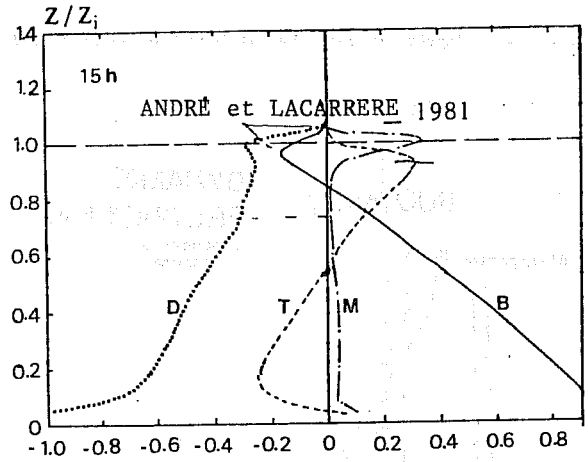

Fig. 12b Normalized balance of turbulent kinetic energy forecast by the model on 2nd at 15.00h.

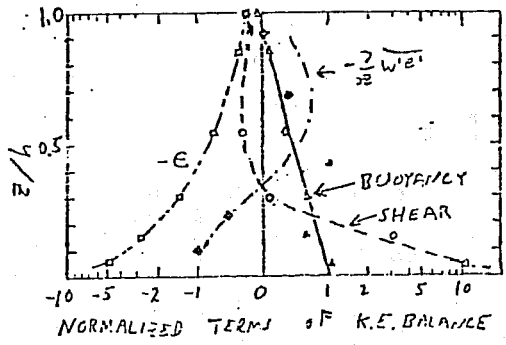

Fig. 12c Terms in the turbulence kinetic-energy balance equation as measured by Pennell and LeMone (1975) over the Carribean Sea just north of Puerto Rico, with $-h/L \equiv 1.5$. Horizontal scale changes from linear to logarithmic at ± 1. Free-convection scaling is used (w_*^3/h on abscissa.

REFERENCES

ANDRE, J.C., G. de MOOR, P. LACARRERE et R. du VACHAT, 1976 a, Turbulence approximation for inhomogeneous flows. Part I The clipping approximation. J. Atmos. Sci. 33, 476-481.

Turbulence approximation for inhomogeneous flows. Part II The numerical simulation of a penetrative convection experiment. J. Atmos. Sci. 33, 482-491.

ANDRE, J.C., G. de MOOR, P. LACARRERE, G. THERRY et R. du VACHAT, 1979, The clipping approximation and inhomogeneous turbulence simulations. Turbulent shear flows I, Springer Verlag, 307-318.

ANDRE, J.C., P. LACARRERE, 1980, Simulation détaillée de la couche limite atmosphérique (simulation détaillée des 2 et 4 juillet 1977 à Voves). La Météorologie VI (n° 22) 5-49.

AUBRY, M., 1975, Etudes de l'atmosphère par sodar. La Météorologie, 35-47.

BUSINGER, J.A., J.C. WYNGAARD, Y. IZUMI et E.I. BRADLEY, 1971, Flux-profile relationships in the atmospheric surface layer. J. Atmos. Sci. 28, 181-189.

COLE, R.S., D.N. ASIMAKOPOULOS, T.J. MOUSLEY and S.J. CAUGHEY, B.A. CREASE, 1980, Some aspects of the construction and use of atmospheric sounders. The ratio and Electronic Engeneer, Vol. 50, 11/12, 587-597.

COANTIC, M. et D. le DUCQ, 1969, Turbulent fluctuations of humidity and their measurement. Radio Sci. 14, 12, 1169-1174.

DEARDORFF, J.W. and G.E. WILLIS, 1974, The computer and laboratory modelling of nonbuoyant particles in the mixed layer. Adv. Geophys. 188, 187-200.

DESJARDINS, R.L. and E.L. LEMON, 1973, Limitations of an Eddy correlation technique for the determination of the carbon dioxide and sensible heat fluxes. Boundary Layer Meteorol., 475-488.

GARRAT, J.R., 1975, Limitations of Eddy correlation technique for the determination of turbulent fluxes near the surface. Boundary Layer Meteorol. 8, 255-259.

GAYNOR, J.E., 1977, Acoustic Doppler measurement of atmospheric boundary layer velocity structure functions and energy dissipation rates. J. Applied Meteorol. 16, 148-155.

GAYNOR, J.E., P.A. MANDICS, A.B. WAHR and F.F. HALL, Jr., 1976, Studies of the tropical marine bondary layer using acousting backscattering during gate, in Preprints of the 17th Radar Meteorology Conference, 303-306, American Meteorological Society,

Boston, Mass.

HEISSAT, J. and C. GERBIER, 1973, Contribution de l'EERM au radiosondage (1-1a) la radiosonde. Etablissement d'Etudes et Recherches Météorologiques. Note 326.

HINZE, J.O., 1975, Turbulence (Mac Graw Hill editor) 2ème édition.

KLAPISZ, C. et A. WEILL, 1978, Modèle semi-empirique d'évolution matinale du profil de vent entre le sol et le sommet de l'inversion. J. Rech. Atmos. 12, 2-3, 113-117.

KOLMOGOROV, A.H., 1941, The local structure of turbulence in an incompressible viscous fluid for very large Reynolds numbers (in Russian), Daklad Akad Nauk SSSR, 30, 301.

MELLING, H. and R. LIST, 1980, Characteristics of vertical velocity fluctuations in the convective atmospheric boundary layer. J. Applied Meteorol. 19, 10, 1184-1195.

PENNEL, W.T. and M.A. LEMONE, 1974, An experimental study of turbulence structure in the fair-weather trade wind boundary layer. J. Atmos. Sci. 31, 1308-1323.

PERRIER, A., B. ITIER, J.M. BERTOLINI and N.B. KATERJI, 1978, A new device for continuous recording of energy balance of natural surfaces. Agric. Meteor. 16, 71-84.

READING, C.J. and D.R. RAYMENT, 1969, The high frequency fluctuations of the wind in the first kilometer of the atmosphere. Radio Sci. 14, 1127-1131.

RUSSEL, P.B., E.E. UTHE et F.L. LUDWIG, 1974, A comparison of atmospheric structure as observed with monostatic acoustic sounder and Lidar techniques. J. Geophys. Res. 79, 36, 5555-5556.

TACONET, O. and A. WEILL, 1981, Vertical velocity field and convective plumes in the atmospheric boundary layer as observed with an acoustic Doppler sodar submitted to B.L.M.

TACONET, O., 1979, Propriétés des plumes convectives dans la couche limite atmosphérique par sondage acoustique Doppler (Thèse de spécialité), Paris VI.

TSVANG, L.R., 1963, Some characteristics of the spectra of temperature pulsations in the boundary layer of the atmosphere. Bull. Acad. Sci. USSR, Geophys. Ser. 10, 1594-1600.

————, 1969, Microstructure of temperature fields in the free atmosphere. Radio Sci. 4, 1175-1177.

WEILL, A., 1977, Mesure des caractéristiques de la turbulence dans la couche limite atmosphérique par sondage acoustique Doppler, Proceeding colloque U.R.S.I., "Propagation dans les milieux contenus", La Baule.

WEILL, A. and F. BAUDIN, 1976, Atmospheric turbulence as observed by in situ measurement and Doppler Sodar, report in Journal of the Acoustical Society of America (Fourth Workshop in Atmospheric Acoustics, San Diego).

WEILL, A., M.E. LEQUERE and P. VAN GRUNDERBEECK, J.P. GOUTORBE, 1978, Measurement of vertical velocity variance by means of an acoustic sounder : Fourth Symposium in Meteo. observations, Published by A.M.S.

WEILL, A., C. KLAPISZ, B. STRAUSS, F. BAUDIN, D. JAUPART, P. VAN GRUNDERBEECK and J.P. GOUTORBE, Measuring heat flux and structure functions of temperature fluctuations with an acoustic Doppler Sodar. J. Applied Meteorol., Vol. 19, 2, 199-205.

WEILL, A., 1981, Sodar micrometeorology : a review 6th symposium of acoustic remote sensing (CALGARY Canada).

WIERINGA, J., 1980, A revaluation of the Kansas mest influence on measurements of stress and cup anemometer over speeding. Boundary Layer Meteorol. 18, 411-430.

WILLIS, G.E. and J.W. DEARDORFF, 1975, Laboratory simulation of the convective planetary boundary layer. Atmos. Technology 7, 80-86.

WYNGAARD, J.C., 1972, in Workshop on micrometeorology on surface layer turbulence, (101-149). Haugen, D.A. (Ed) (American Meteorological Society, Boston, Mass).

WYNGAARD, J.C. and O.R. COTE, 1971, The budgets of turbulent kinetic energy and temperature variance in the atmospheric surface layer. J. Atmos. Sci. 28, 190-201.